Geophys. J. Int. (1996) **127**, 503–514

Magnetobiostratigraphy of the Spathian to Anisian (Lower to Middle Triassic) Kçira section, Albania

Giovanni Muttoni,[1,2] Dennis V. Kent,[1] Selam Meço,[3] Alda Nicora,[2] Maurizio Gaetani,[2] Marco Balini,[2] Daniela Germani[2] and Roberto Rettori[4]

[1] *Lamont-Doherty Earth Observatory, Palisades* 10964 NY, *USA*
[2] *Dipartimento di Scienze della Terra, via Mangiagalli* 34, 20133 *Milan, Italy*
[3] *Fakultety Geolojia i Miniera, Polythekniki Universiteti, Tirana, Albania*
[4] *Dipartimento di Scienze della Terra, Piazza Universitá,* 06100 *Perugia, Italy*

Accepted 1996 July 18. Received in original form 1996 March 26

SUMMARY

Magnetobiostratigraphic data are presented from three Early/Middle Triassic Han-Bulog Limestone successions from Kçira, northern Albania. A total of 206 standard palaeomagnetic samples were obtained for thermal demagnetization and statistical analysis from the 42, 10 and 5 m thick sections. The reversal-bearing characteristic component, carried by haematite and magnetite, defines a composite sequence of six main polarity intervals (Kç1n to Kç3r) in which are embedded four short polarity intervals, one at the base of Kç1n and three towards the top of Kç1r. The early acquisition of the characteristic remanence is supported by the lateral correlation of magnetozones between sections. The Early/Middle Triassic boundary, approximated by the first occurrence of the conodont *Chiosella timorensis*, falls close to the Kç1r/Kç2n polarity transition. This is in good agreement with recently published magneto-biostratigraphic data from the coeval Chios (Greece) sections. The palaeomagnetic pole calculated from the Kçira characteristic directions lies close to the Triassic portion of the apparent polar wander path for Laurussia (in European coordinates). However, a 40–45° clockwise rotation of the external zone of the Albano–Hellenic Belt to the south of the Scutari–Pec Line is thought to have occurred since the Early–Middle Miocene. The Kçira pole acquires a West Gondwana affinity when restored for the Neogene clockwise rotation. If the clockwise rotation was entirely related to Neogene tectonics, the Kçira area was evidently associated with West Gondwana and located at 12–16°N of the western Tethys margin.

Key words: Albania, biostratigraphy, magnetostratigraphy, Triassic.

INTRODUCTION

Significant progress has been made in recent years in constructing a Triassic geomagnetic polarity sequence correlated with biostratigraphic and chronostratigraphic data in Tethyan marine sections (e.g. Gallet *et al.* 1992, 1993, 1994; Muttoni *et al.* 1994; Graziano & Ogg 1994; Muttoni, Kent & Gaetani 1995). A polarity sequence across the Early/Middle Triassic boundary was recently obtained from the ammonoid- and conodont-bearing Marmarotrapeza Formation on Chios, Greece (Muttoni *et al.* 1995). However, the fossiliferous Tethyan limestone sections are often condensed and replication is needed to be sure that the magneto- and biostratigraphic representation is complete. To confirm the Chios result, a Lower/Middle Triassic Han-Bulog Limestone succession from Kçira, northern Albania, was studied. We were able to obtain a magnetostratigraphic framework for the vertical distribution of ammonoids, conodonts and benthic foraminiferas. A detailed geological map of the Kçira sections area is also provided.

GEOLOGY

The area of Kçira in northern Albania (Fig. 1a,b) has been known to geologists since the beginning of this century. Arthaber (1911) and Nopcsa (1929) carried out pioneering work in the region, describing an Early Triassic ammonoid fauna within the reddish nodular Han-Bulog Limestone succession. During the 1960s and 1970s, extensive field work resulted in the production of a 1:250 000 geological map of the Kçira and surrounding regions with explanatory notes in Albanian (ISPGJ–ISGJN 1982, 1983). Additional reports (e.g.

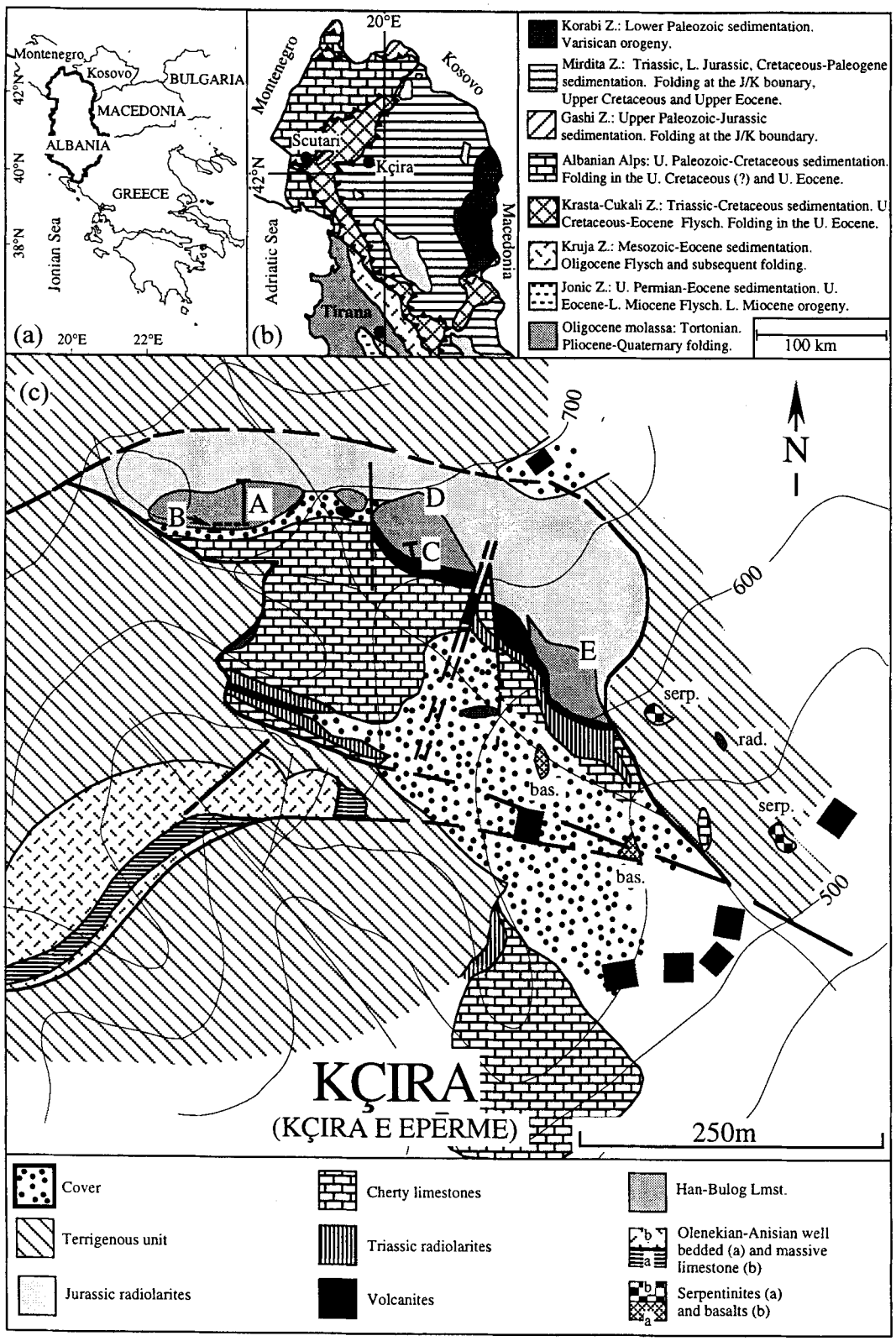

Figure 1. (a) Geographical location of Albania in the Balkan peninsula. (b) Simplified geological map of northern Albania. The Kçira sections are located in the External Mirdita Zone. (c) Geological map of the Kçira area. 'A', 'B' and 'C' are sections KçA, KçB and KçC; 'D' and 'E' designate sites of palaeontological or lithological interest described in the text.

Kodra 1987, 1988) and PhD theses (e.g. Godroli 1992) were also produced.

Tectonically, the area of Kçira belongs either to the External Mirdita Subzone (Shallo 1992, 1994) or to the equivalent Subzone of Qerret–Miliska (Godroli, 1992; Kellici, De Wever & Kodra 1994). Both subzones consist of a belt of carbonate, volcanic and radiolarite blocks embedded in a thick volcaniclastic and terrigenous unit (e.g. Fig. 1c) and bounded by thrust slabs of ultrabasites. These blocks range in size from a few metres to a few kilometres and may preserve a coherent Triassic to Jurassic stratigraphy (Gaetani *et al.*, in preparation). The terrigenous unit [the 'Flysch précoce' of Godroli (1992), equivalent to the 'Volcano-Sedimentary Formation' of Beccaluva *et al.* (1994)] is thought to be of Late Jurassic to Early Cretaceous age (Shallo 1992, 1994); the presence of Permian clastics is assumed, but has not been palaeontologically proved (Kellici *et al.* 1994). We propose that the terrigenous unit was the accretionary wedge resulting from the subduction of the Mirdita ocean below the Korabi microplate. The blocks are thus interpreted as remnants of the rift shoulders that bordered the incipient Mirdita ocean, and which are now tectonically embedded within the accretionary wedge. The Krasta–Cukali Zone is interpreted as the rim basin located between the Mirdita rift shoulders and the passive margin of the Ionian Zone *sensu lato*. The Korabi, Mirdita and Krasta–Cukali zones correspond in the Hellenides to the Pelagonian, Othrys–Subpelagonian and Pindos–Olonos zones, respectively (Kellici *et al.* 1994; see also Robertson *et al.* 1991; Godroli 1992).

The Kçira area is characterized by a set of blocks containing a stratigraphically coherent Early to Middle Triassic Han-Bulog Limestone succession associated with Triassic to Jurassic carbonate and volcanic rocks (Fig. 1c; Gaetani *et al.*, in preparation). The Han-Bulog succession, presently disrupted along strike, probably formed a single slab prior to being embedded in the terrigenous unit, and possibly also during later times, if its disruption is to be ascribed only to the effects of Alpine tectonics.

Two sections were studied for magnetobiostratigraphy (KçA and KçB) and a third section (KçC) was sampled only for magnetostratigraphy (Fig. 1c). The KçA and KçB sections are most likely the localities described by Nopcsa (1929). Bedding attitude varies with strikes/dips from 347°/34°E at KçA to 12°/45°E at KçB and KçC.

LITHOLOGY

The KçA and KçB sections are a few metres apart within the same general outcrop but are not visibly connected (Fig. 1c). KçB is about 4.5 m thick, and on the basis of projecting the layers partially overlaps with the basal portion of KçA, which is about 42 m thick (Fig. 2). Both sections are comprised of the Han-Bulog Limestone, consisting of reddish to pale-pink wackestones and mudstones arranged in thin nodular beds that are strongly amalgamated to form metre-scale composite layers. The basal 5 m of KçA (as well as the entire KçB) are reddish and clay-rich, with pervasive bedding-parallel stylolites, whereas the overlying 37 m are more pink to pale pink in colour and consist of strongly recrystallized and amalgamated beds. A set of cm-thick calcite veins cuts the bedding between 18 and 23 m. The uppermost few metres, sometimes also containing packstones, are richer in bioclasts and more distinctly bedded (Fig. 2). The top of the Han-Bulog Limestone (e.g. Fig. 1c, site D) is marked by the presence of small neptunian dykes sealed by a cm-thick silicified crust, and overlain by radiolarites whose age is interpreted as Middle Jurassic on the basis of correlation with other sections in the Qerret–Miliska Subzone (Kellici *et al.* 1994).

The KçC section is 10.2 m thick and constitutes a separate outcrop located a few tens of metres east of KçA and KçB (Fig. 1c). Although a detailed lithological description was not made of KçC, an up-section decrease in pigmentation from reddish to pink, which closely resembles that observed at KçA (Fig. 2), provides a first-order means of lithological correlation.

BIOCHRONOLOGY

Samples for palaeontological dating were taken only from sections KçA and KçB, but provided ammonoids (studied by MB and DG), conodonts (SM and AN) and benthic foraminifera (RR) of biochronological significance (see also Gaetani *et al.*, in preparation).

Ammonoids are concentrated in the basal portion of the Han-Bulog Limestone. Rare specimens were also collected in the middle and upper parts of section KçA. Levels AK2bis and AK5 from section KçA (Fig. 2) contain *Subcolumbites, Albanites, Procarnites, Pseudosageceras, Leiophyllites* and *Eophyllites*. Level AK2bis may be directly correlated to level AK62 of section KçB. This assemblage, largely corresponding to the fauna described by Arthaber (1911), is of Spathian age and belongs to the Prohungarites–Subcolumbites zone *sensu* Kummel (1969). Orchard (1995) also ascribed the Prohungarites–Subcolumbites beds of North America to the middle Spathian. In the middle part of section KçA (samples AK31, AK36, AK38, AK40), small specimens of smooth-shelled ammonoids belonging to the long-ranging genus *Procarnites* and to other genera of the family Ussuritidae were collected. Finally, the uppermost Han-Bulog Limestone yielded the Anisian ammonoids *Sturia* (in section KçA, Fig. 2), *Ptychites* and *Monophyllites* (at site E, Fig. 1c). Ammonoid biostratigraphy points to a middle Spathian age for section KçB and for the base of section KçA, and a generic Anisian age for the top of section KçA.

Conodonts provide a better tool for biostratigraphy as most of the samples contain specimens that are age-diagnostic to the substage level. The following assemblages and/or events are recognized (Fig. 2). (1) The basal 21.8 m of section KçA (samples AK1 to AK29) contains *Neospathodus symmetricus* and *N. homeri*, the latter ranging up to a maximum of 25.5 m in the section (AK35). *N. abruptus* is confined to the basal 1.25 m of section KçA, and may extend downwards to section KçB for an additional 2 m. *N. brochus* is also confined to the basal 2.25 m of section KçA, with an isolated occurrence at 21.8 m (sample AK29). This assemblage is similar to that descibed for the middle Spathian by Orchard (1995, fauna #3 in Fig. 1). (2) The middle–upper part of section KçA is characterized by the presence of short-lived species of gondolellids. *Neospathodus gondolelloides* appears at 20.2 m (AK28), followed by the appearance of *Chiosella timorensis* (22.4 m, AK30). This is in agreement with data from Chios (Gaetani *et al.* 1992; Muttoni *et al.* 1995). The appearance of *Chiosella timorensis* (*Gondolella timorensis* in Gaetani *et al.* 1992 and Muttoni *et al.* 1995) may be used to approximate the base of the Anisian when ammonoids are absent. *Gondolella bulgarica* appears at 28.7 m (AK40) and is a proxy for the base of the Bithynian

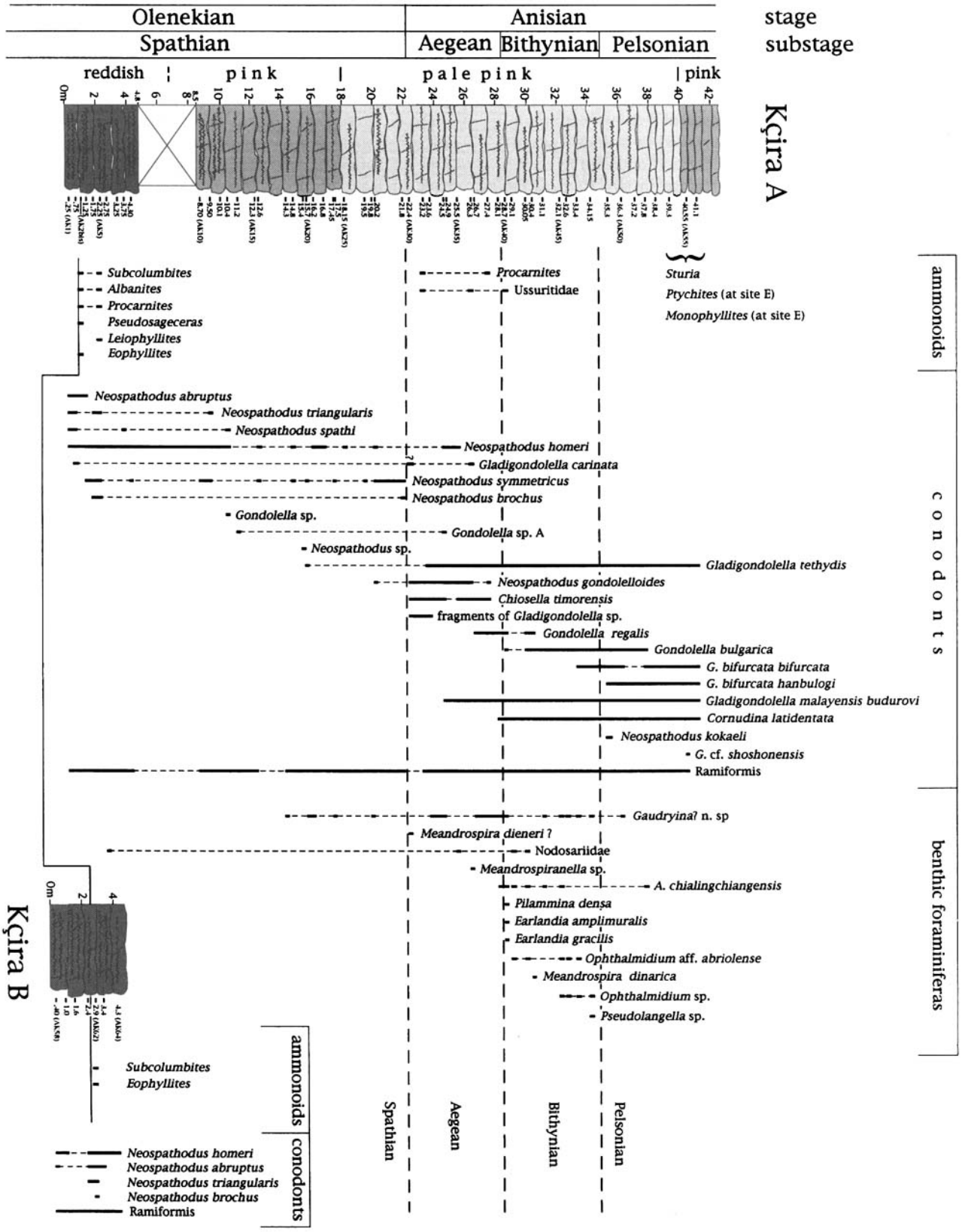

Figure 2. Ammonoid, conodont and benthic foraminifera biostratigraphy of the middle Spathian to basal Pelsonian KçA section and middle Spathian KçB section.

(i.e. the second substage of the Anisian) according to Nicora (1977), Kovacs & Kozur (1980) and Sweet (1988). *Neospathodus kokaeli* appears at 35.3 m (AK49) and approximates the base of the Pelsonian (i.e. the third substage of the Anisian) according to Kovacs & Kozur (1980) and Sweet (1988). Section KçA thus covers the middle Spathian to basal Pelsonian time-interval, whereas section KçB is restricted to the middle Spathian. The vertical sequence of the biochronological events does not appear to have been altered by major primary or secondary processes, e.g. sedimentation gaps or faulting.

Foraminifera are very scarce in the lower part of section KçA (Fig. 2). *Gaudryina*? n. sp. is discontinuously present from 14.3 m (AK17) to 22.4 m (AK30), where *Meandrospira dieneri*? appears. A more diversified and abundant fauna was recovered from 28.1 to 34.2 m (samples AK39 to AK48). This assemblage is characterized by *Ophthalmidium* aff. *abriolense, Arenovidalina chialingchiagensis, Pilammina densa, Meandrospira dinarica, Meandrospiranella* sp., *Earlandia amplimuralis* and *E. gracilis*. An Anisian age not younger than Pelsonian is ascribed to this assemblage. Of note is the presence of *P. densa* in association with conodonts of Bithynian age.

PALAEOMAGNETIC PROPERTIES

Samples were collected with a portable water-cooled rock drill and oriented with a magnetic compass. Sections KçA and KçB were sampled at an average sampling interval of 20–25 cm, with slightly coarser sampling (40–50 cm) at KçC. Each 2.5 cm diameter core sample yielded one and occasionally two standard 11cc specimens, giving a total of 206 specimens for analysis. Thermal demagnetization treatments and measurements of natural remanent magnetization (NRM) were performed in a shielded room (where the ambient magnetic field was less than 300 mT). Heating and cooling were carried out in a well-shielded demagnetizer in which ambient fields were less than 5 nT. Magnetic remanences were measured with a 2G Model 760 three-axis cryogenic magnetometer. After each thermal demagnetization step, the initial magnetic susceptibility of each specimen was measured with a Bartington MS2 susceptibility bridge to monitor any mineralogical alteration resulting from the heating procedure. Least-squares analysis (Kirschvink 1980) was used to determine the component directions of NRM, chosen by inspection of vector end-point demagnetograms (Zijderveld 1967). Mean directions were determined with standard Fisher statistics.

Interpretable palaeomagnetic directions were obtained from 183 out of 206 specimens (Fig. 3, Table 1); the remaining 23 specimens gave mainly univectorial trajectories of various directions interpreted as lightning-induced remanences. Between room temperature and about 200 °C, 84 per cent of the Kçira specimens yielded a low unblocking temperature component with *in situ* northerly declinations and downward inclinations ranging between about 50° and 60°. This component is probably of viscous origin and is consistent with acquisition along the present-day field at Kçira where the present geomagnetic (or the expected time-averaged dipole) field is inclined at 59° (or 61°). In the temperature range between about 400 °C and either 520–575 °C or 650–680 °C, a characteristic ('Ch') component with either northeast-and-down or southwest-and-up directions was resolved in 88 per cent of the samples. Over intermediate unblocking temperatures of about 200 °C to 400 °C there are often transitional directions tentatively interpreted as being due to overlap between the present-day field and the 'Ch' components. Five samples from KçB show, however, well-grouped south-and-up trajectories unblocked between 200 °C and 400 °C (e.g. Fig. 3, sample 2kc2.30). These magnetizations may have been acquired during a geologically recent reversed geomagnetic polarity interval, although the mean value of the *in situ* inclination (−72.5°) is some 10° steeper than would be expected from a recent field.

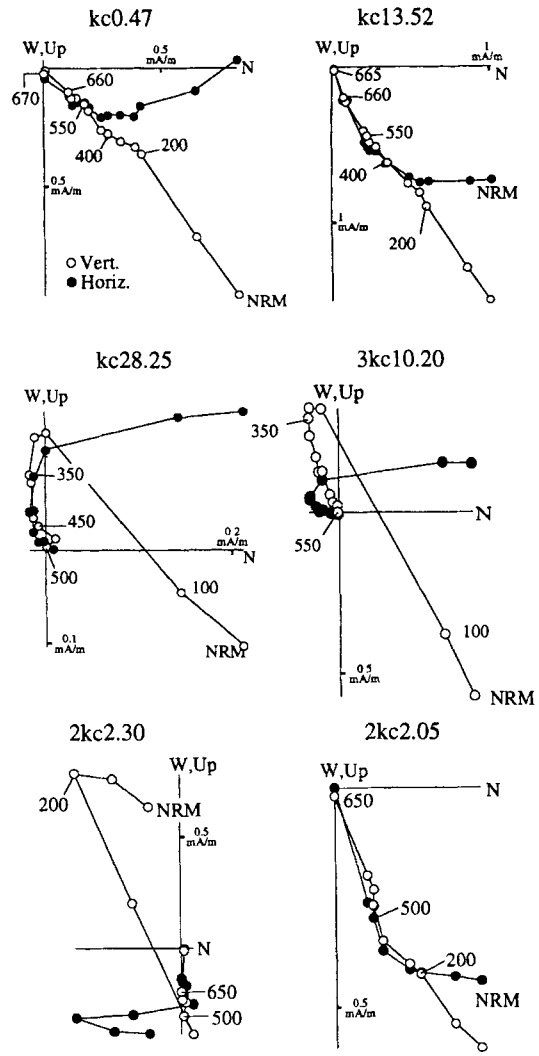

Figure 3. Zijderveld thermal demagnetograms of NRM of representative samples of Han-Bulog Limestone from Kçira. Closed symbols are projections onto the horizontal plane and open symbols are projections onto the vertical plane in *in situ* coordinates. Demagnetization temperatures are in °C.

The 'Ch' component has dual polarity at all three sites (Fig. 4a; Table 1). A mean characteristic direction was calculated for each site, as well as for each separate rock outcrop (i.e. KçA + KçB and KçC). Both the three site-mean and the two outcrop-mean directions show some degree of convergence after correction for bedding tilt (Fig. 4b, c); the precision parameter increases by factors of 3 and 3.8 respectively, with a full (100 per cent) tilt correction, suggesting that the characteristic remanence was acquired before the main phase of deformation in the country rock (i.e. in pre-Cretaceous to

Table 1. Palaeomagnetic directions from Kçira A, B and C sections.

			In Situ Directions				Tilt Corrected Directions						
Section	Comp.	N/n	k	a95(°)	Dec.(°)	Inc.(°)	k	a95(°)	Dec.(°)	Inc.(°)	Lat./Long.(°)	dp/dm(°)	Plat.(°N)
KçA	Ch	165/145	8	4.3	52.1	43.5	8	4.3	32.4	24.5	49.5/146.5	2.5/4.6	12.8
KçB	South-up	017/005	94	7.9	172.6	-72.5	95	7.9	183.9	-28.1			
KçB	Ch	017/016	22	7.7	76.8	54.0	22	7.7	46.1	24.2	40.5/132.4	4.4/8.2	20.5
KçC	Ch	024/022	16	8.0	85.6	58.2	16	8.0	46.7	30.9	42.9/128.0	5.0/8.9	16.6
mean specim.	Ch	206/183	8	3.8	59.6	46.9	9	3.7	37.8	26.0	46.8/139.5	2.1/3.9	13.7
mean sites	Ch	3 sites	38	20.4	69.6	52.8	98	12.5	41.7	26.7	44.6/135.2		14.1

Notes. Comp.: component designation (Ch is the characteristic component); N: number of core samples collected in the field, n: number of core samples (= number of 11 cc specimens) used in statistical analysis; k: precision parameter; a95: half-angle of cone of 95 per cent confidence about the mean direction; Dec., Inc.: declination and inclination; Lat., Long.: latitude (°N) and longitude (°E) of the palaeomagnetic pole; dp/dm: semi-axes of the confidence oval about the palaeomagnetic pole; Plat.: palaeolatitude.

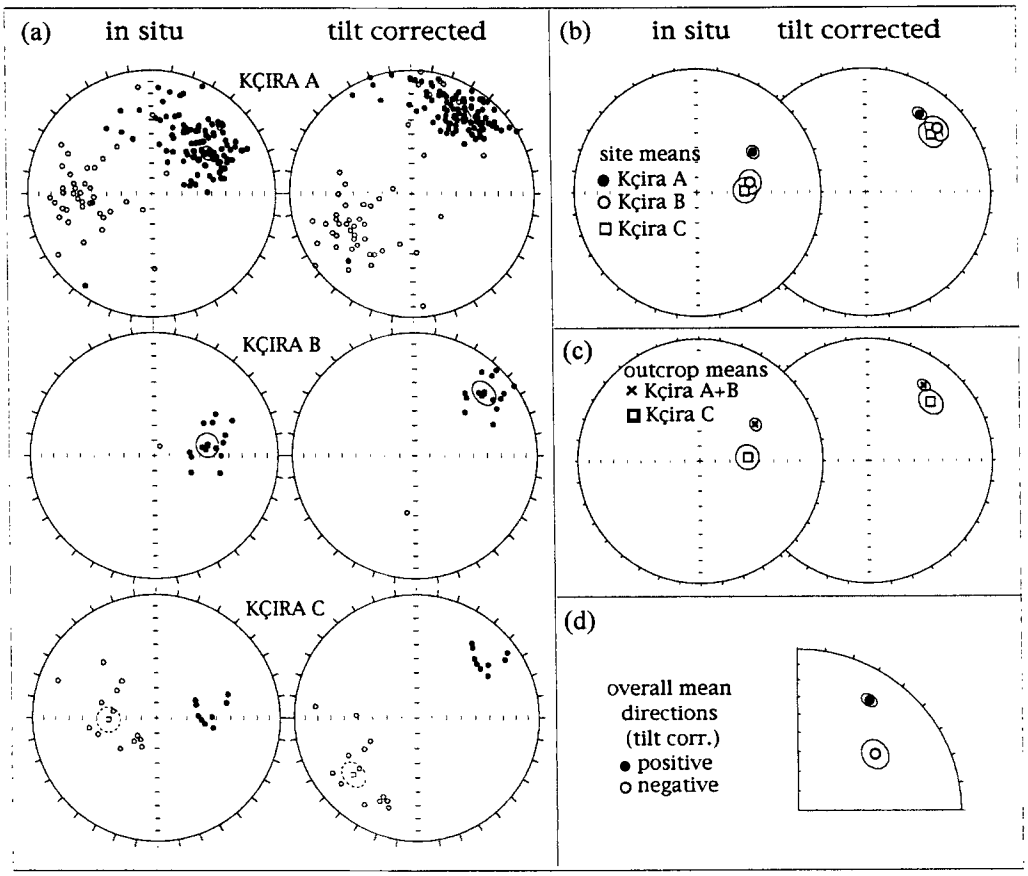

Figure 4. Equal-area projections before (*in situ*) and after bedding tilt correction of the characteristic component directions according to (a) samples at each site, (b) site means, (c) outcrop means and (d) overall positive and negative mean directions.

Cenozoic times). However, the limited difference in bedding attitudes makes the fold test statistically inconclusive.

The 183 normal and reversed polarity directions from all the sites deviate from antipodality by 26.7° or 27.5° in *in situ* or tilt-corrected coordinates, respectively (Fig. 4d). Only at site KçC do the normal and reversed directions pass the reversal test at the 95 per cent level of confidence, classified as 'C' according to the criteria of McFadden & McElhinny (1990). The general departure from antipodality may be due to contamination of the characteristic magnetizations by the present-day field component or perhaps by an intermediate unblocking temperature component that was poorly resolved and tentatively attributed to overlapping demagnetization spectra. In any case, we assume that the contamination influences both the normal and reversed directions, whose averaging by inverting to common polarity should minimize the biasing effect in determining an overall mean direction. The characteristic 'Ch' component in bedding coordinates has a mean direction of Dec = 37.8°, Inc = 26.0° ($a_{95} = 3.7°$, $k = 9$, $N = 183$; Table 1), and, provided it was acquired early in the depositional history, indicates an Early/Middle Triassic palaeolatitude of about 14°N for the Kçira region.

ROCK MAGNETIC PROPERTIES

The ferromagnetic phases were investigated by means of thermal unblocking characteristics of orthogonal-axes isothermal remanent magnetization (IRM) according to the method of Lowrie (1990) (Fig. 5a). The basal 18 m at KçA are reddish in colour and, not surprisingly, are dominated by a high coercivity/680 °C maximum unblocking temperature phase interpreted as haematite. The overlying pink to pale-pink limestones are dominated by a low coercivity/575 °C maximum unblocking temperature phase compatible with magnetite, coexisting with subsidiary haematite. The change in magnetic mineralogy can be quantitatively portrayed by the initial IRM high/low (0.12 T/1.2 T) coercivity phase ratio, which is less than one (i.e. dominance of haematite) in the lower part of the section and progressively increases (i.e. higher magnetite to a haematite ratio) upsection (Fig. 5b). The stratigraphic distribution of unblocking temperature spectra of the characteristic 'Ch' component conforms to these bulk rock-magnetic properties (Fig. 5c). Maximum unblocking temperatures of 680 °C are confined to within the basal 18 m of the KçA section, whereas above this level they decrease to below 600 °C; a correlative decrease occurs also at KçC.

The basal haematite-rich levels represent the juvenile stage of the Han-Bulog basin, which was characterized by low sedimentation rates, as evidenced by the highly nodular texture of the rock and the presence of pervasive stylolitization. Persistent oxidizing conditions presumably triggered the growth of abundant haematite, contributing to the relatively high NRM and susceptibility intensities in this part of the section (Fig. 5d,e). Later in the depositional history, more reducing conditions, perhaps related to higher sedimentation rates, allowed the preservation of some magnetite coexisting with less-abundant haematite. The magnetite–haematite mixture is evidently well diluted within the sediment giving rise to lower NRM and susceptibility intensities, although the lowest values between 18 and 23 m in the KçA section are also associated with a dense network of calcite veins (Fig. 5d,e). Finally, the uppermost few metres of the Kçira succession are even richer in resedimented carbonate layers that might have enhanced the concentration of detrital magnetite.

The mean characteristic directions from the basal haematite-bearing beds and the overlying magnetite-dominated beds are statistically indistinguishable at the 99 per cent level of confidence according to the criteria of McFadden & Lowes (1981). This correspondence is consistent with a time of acquisition for the characteristic remanence carried by either haematite or magnetite very early in the depositional history of the Han-Bulog Limestone.

MAGNETIC STRATIGRAPHY

A virtual geomagnetic pole (VGP) was calculated for each sample characteristic component direction after correction for bedding tilt. The latitude of the sample VGP with respect to the overall mean (north) palaeomagnetic pole was used to delineate the magnetic polarity stratigraphy. VGP relative latitudes approaching +90°N (−90°N) are interpreted as recording normal (reversed) polarity. For polarity magnetozone identification, we adapt the nomenclature used by Kent, Olsen & Witte (1995) for the Late Triassic/earliest Jurassic Newark geomagnetic polarity sequence. Successive pairs of predominantly normal and predominantly reversed polarity intervals are assigned an integer in ascending order from base to top. Attached to each ordinal number is the prefix 'Kç' for the locality and the suffix 'n' or 'r' that identifies the magnetizone as normal or reverse polarity, respectively. Any shorter polarity intervals within a magnetozone can be identified by successive integers (ascending up-section) appended after a decimal point to the magnetozone designation of higher rank, again with a suffix indicating normal or reversed polarity.

At KçA, the VGP relative latitudes define a sequence of six main polarity intervals (Kç1n to Kç3r) in which are embedded four short polarity intervals, one at the base of Kç1n and three towards the top of Kç1r (Fig. 6). The Kç1n/Kç1r boundary is placed at 17 m and thus does not coincide with the change in dominant magnetic mineralogy that occurs 1 m above. Normal and reversed magnetic polarity intervals therefore appear to be carried by both haematite and magnetite. A short reversed polarity interval located near the base of KçA correlates with the short reversed polarity interval at 2.60 m in KçB giving credibility to these single sample reversals. Finally, the magnetic polarity stratigraphy at KçC encompasses the uppermost part of the normal polarity interval Kç1n and most of the succeeding reversed interval Kç1r. The good match of the polarity stratigraphy between KçC and KçA also confirms the presence of the short polarity intervals detected towards the top of Kç1r in both sections.

DISCUSSION AND CONCLUSIONS

The magnetobiostratigraphy across the Early/Middle Triassic (Spathian/Aegean) boundary from Chios (Greece) was studied in two sections (A + C + D and G; Muttoni *et al.* 1995) of the Marmarotrapeza Formation, which consists of a red nodular limestone facies very similar to the Han-Bulog Limestone of Kçira. The Chios magnetic stratigraphy consists of a normal (Chios A+) to reverse (Chios B−) to normal (Chios C+) polarity sequence; the Early/Middle Triassic boundary was placed in the lowest part of Chios C+ at the first occurrence of the ammonoid species *Aegeiceras ugra, Paracrochordiceras* spp., *Paradanubites depressus* and *Japonites* sp., which define the Aegeiceras–Japonites beds (Fig. 7). This ammonoid assemblage slightly post-dates the first occurrence of the conodont *Chiosella timorensis* (*Gondolella timorensis* in Muttoni *et al.* 1995). The first occurrence of *Chiosella timorensis* was thus regarded as a good proxy for the Early/Middle Triassic boundary when ammonoids are absent, e.g. at Kçira (Gaetani *et al.* 1992; Muttoni *et al.* 1995).

There is a good match between Kçira and Chios in the pattern of polarity reversals across the Early/Middle Triassic boundary based on the first occurrence of *Chiosella timorensis*: magnetic polarity intervals Chios A+ and Chios B− correlate with Kç1n and Kç1r, whereas Chios C+ most probably corresponds to Kç2n (Fig. 7). Muttoni *et al.* (1995) highlighted the presence of a fault and a hard ground at the Chios B−/Chios C+ transition at sections A + C + D and G, respectively. Both discontinuities, however, were regarded as not particularly important because the ammonoid zones were in correct stratigraphic superposition. A gap of a few metres in the Chios record is now apparent, however, as inferred by the absence of the short polarity reversals that are present at Kçira at the top of polarity zone Kç1r (Fig. 7). Consequently, the expected level of the Early/Middle Triassic boundary in the more

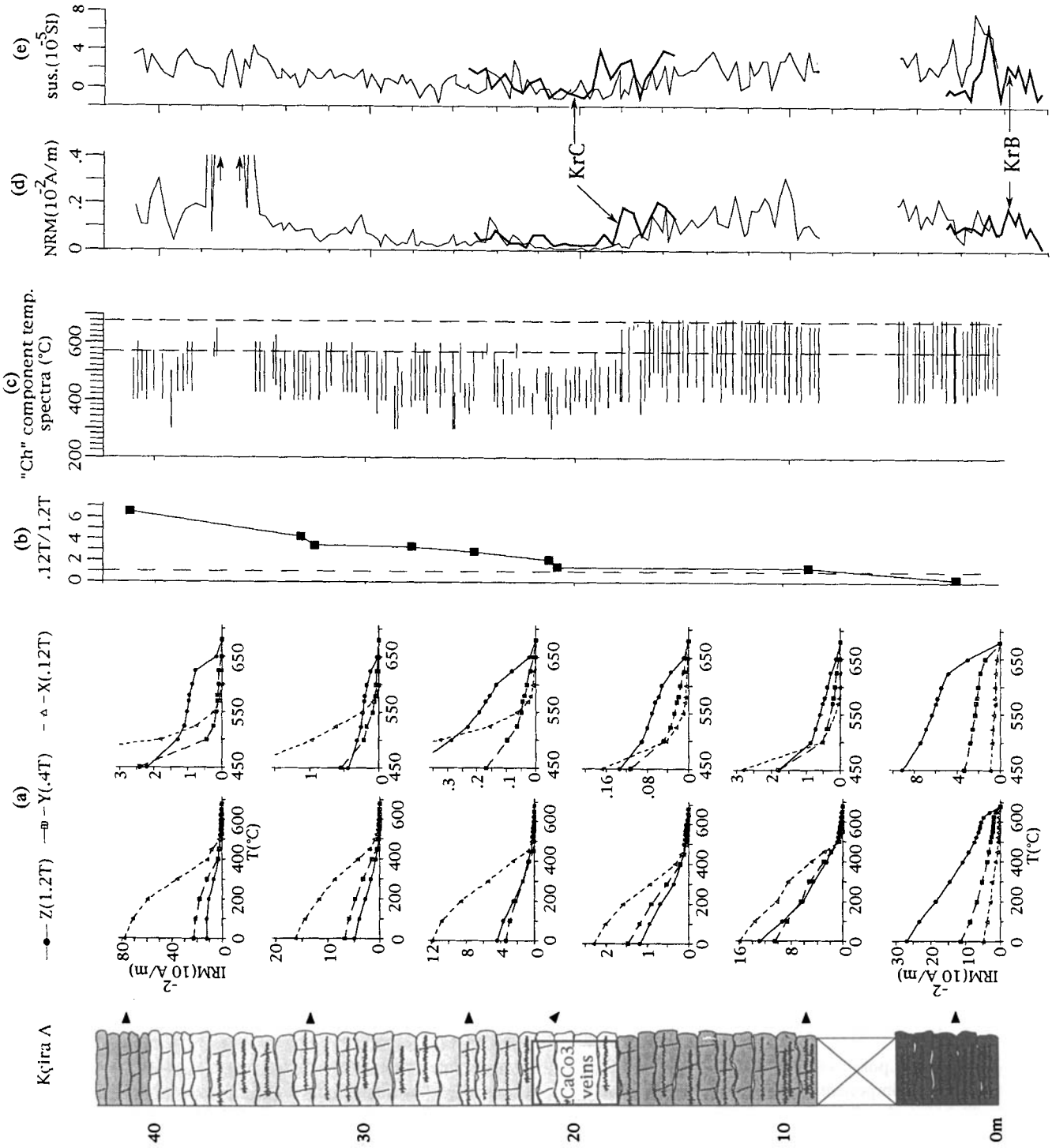

Figure 5. Variation of rock magnetic properties in the KçA section. (a) Thermal decay for representative KçA samples of three-axis IRM obtained by inducing a 1.2 T field along the *z*-axis, 0.4 T along the *y*-axis and 0.12 T along the *x*-axis. (b) Ratio of soft to hard IRM (0.12 T/1.2 T). (c) Unblocking temperature spectra of the characteristic 'Ch' component. (d) Intensity of NRM. (e) Initial (volume) susceptibility. NRM and susceptibility values for KçB and KçC are shown by bold curves.

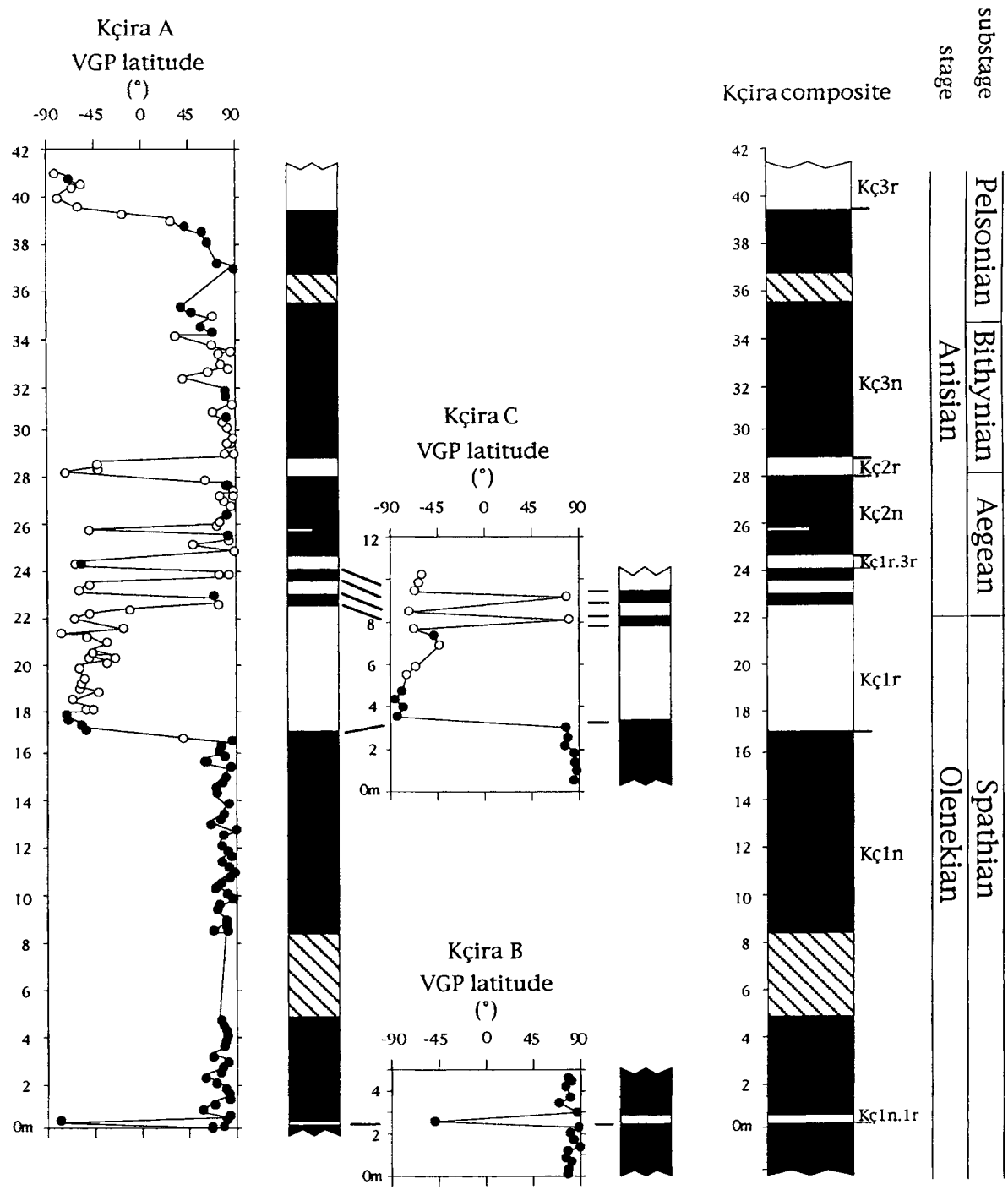

Figure 6. Relative VGP latitudes of the characteristic component as a function of stratigraphic position with polarity interpretation for the Kçira sections. Filled (open) circles are VGP relative latitudes of the characteristic remanence carried by haematite (mainly magnetite). Magnetic polarity zones are shown by filled (open) bars for normal (reversed) polarity; single-sample polarity zones are shown by half-bars.

complete Kçira sequence, based on the projected stratigraphic position of the Aegeiceras–Japonites ammonoid beds from Chios, should be a few metres above that based on the conodont *Chiosella timorensis*. Such an ammonoid-based Early/Middle Triassic boundary would imply that the Aegean substage is very restricted in duration and hardly distinguishable from the overlying Bithynian.

The characteristic directions at Kçira define a palaeomagnetic pole located at 46.8°N, 139.5°E (dp = 2.1°, dm = 3.9°, $N = 183$) (Table 1). The Kçira pole lies close to the Triassic portion of the Early Permian to Early Jurassic apparent polar wander path (APWP) for Laurussia (in European coordinates) (Fig. 8). However, Speranza *et al.* (1995) and Mauritsch *et al.* (1995) report a 40–45° clockwise rotation of the external zone of Albania to the south of the Scutari–Pec Line since the Early–Middle Miocene. Speranza *et al.* (1995) infer that the external

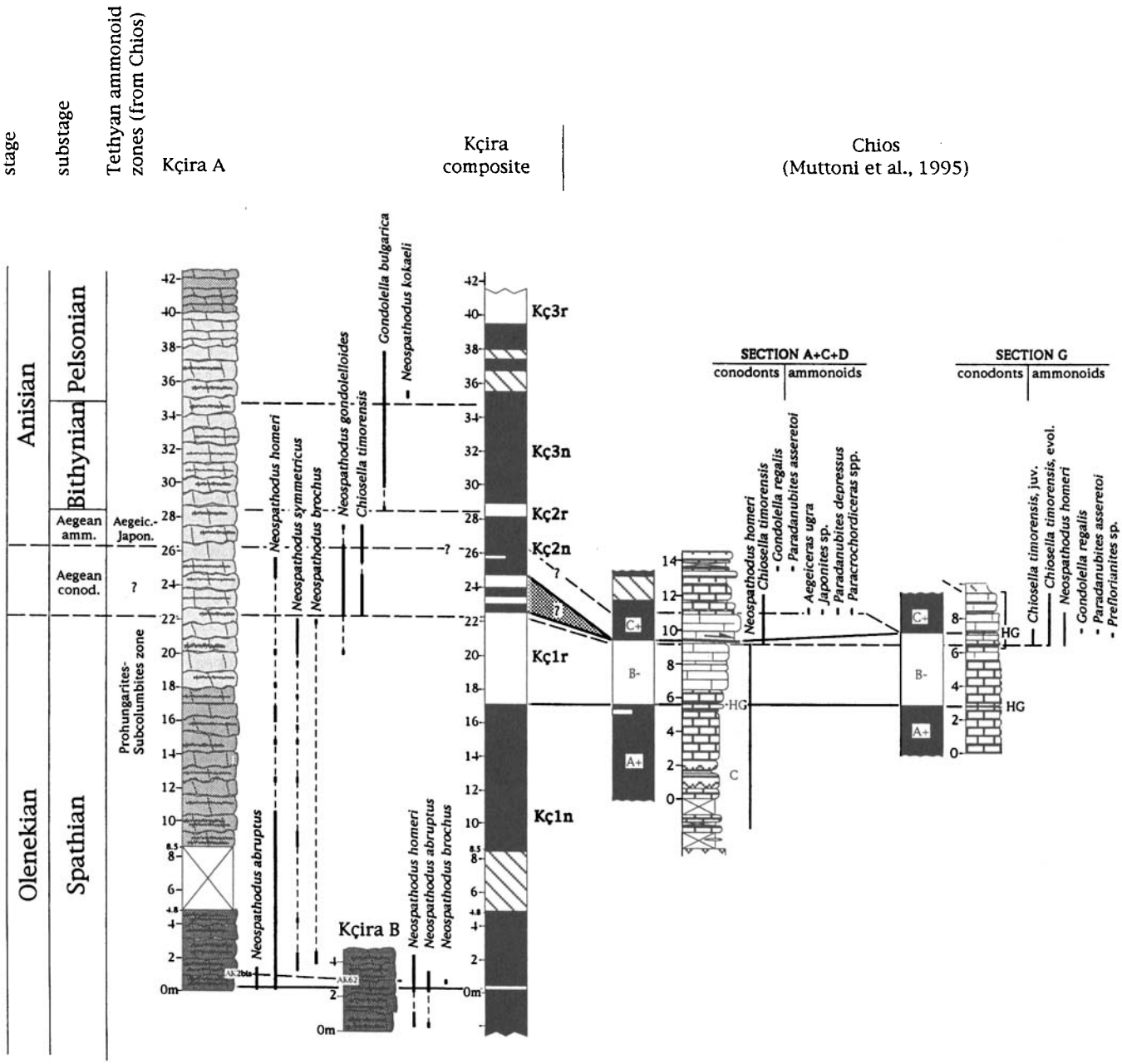

Figure 7. Comparison of magnetobiostratigraphic sequences from the Kçira composite and the Chios sections of Muttoni *et al.* (1995). Solid lines of correlations are for magnetic polarity zones, dashed lines for biostratigraphic events. In the Chios sections, 'HG' is hard ground and 'C' is a condensed interval. Note the presence of a gap of a few metres in the Chios record compared to Kçira (shaded area), accounted for by a fault at the ChiosB−/ChiosC+ boundary in section A + C + D, and presumably the hard ground near the top of ChiosB− in section G. Two options for the Early/Middle Triassic boundary are discussed in the text, namely at the first occurrence of the conodont *Chiosella timorensis* or at the first occurrence of the ammonoids *Aegeiceras ugra, Paracrochordiceras* spp., *Paradanubites depressus* and *Japonites* sp., which define the Aegeiceras–Japonites beds.

zones of the Albano–Hellenic Belt rotated virtually as a single entity from the Peloponnesus to northern Albania. The Kçira pole, when restored for the Neogene 40–45° clockwise rotation, acquires a West Gondwana affinity (Fig. 8). We therefore conclude that the Kçira area was most probably associated with West Gondwana during the Early/Middle Triassic.

We infer that Kçira was located at about 12–16°N on the western passive continental margin (i.e. the Mirdita–Othrys–Subpelagonian Zone) of the Korabi–Pelagonian microplate that rifted off the Adria–Africa margin (i.e. the Ionian Zone *sensu lato*) during the Triassic (Fig. 9). The opening of the Cukali–Pindos–Olonos seaway, which is interpreted as the forerunner of a southern arm of the Neotethys that brought into existence the Korabi–Pelagonian microplate, is apparently not resolvable by the available palaeomagnetic data. It is worth noting that the Early/Middle Triassic palaeopole from Chios, coeval with the Kçira palaeopole, experienced an approximately 70° counterclockwise rotation with respect to

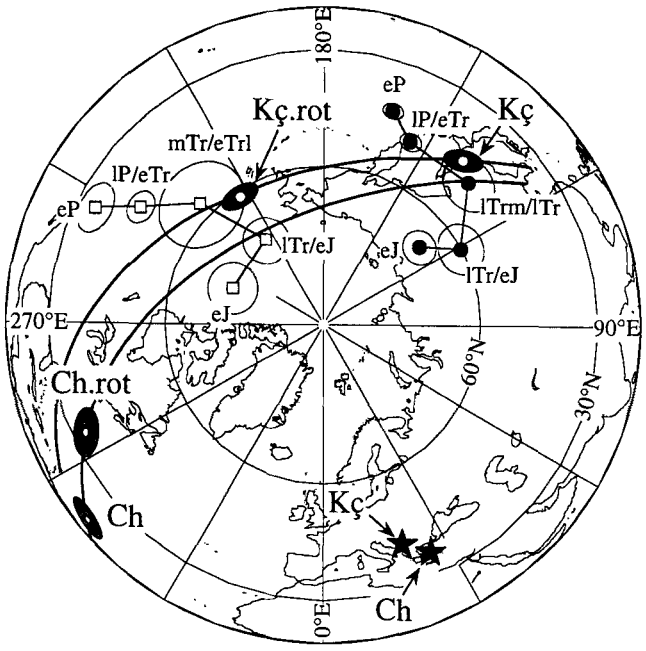

Figure 8. Apparent polar wander paths for Laurussia in European coordinates (solid circles) and for West Gondwana in northwest African coordinates (open squares) [Muttoni, Kent & Channell (1996) and references therein], compared to the poles calculated from the characteristic components isolated at Kçira (Kç) and Chios (Ch; Muttoni *et al.* 1995). Also shown are the Kçira palaeopole restored for the Neogene 45° clockwise rotation (Kç.rot) of Speranza *et al.* (1995), and the Chios palaeopole restored for a counterclockwise rotation of 25° of presumed similar age (Ch.rot) as described by Muttoni *et al.* (1995) and references therein. The small circles through the unrotated and rotated Kçira and Chios poles represent the copalaeolatitudes calculated from the Kçira and Chios characteristic component directions and represent the expected locus of palaeopoles resulting from tectonic rotations about local vertical axes. Age symbols are as follows. eP: Early Permian; lP/eTr: Late Permian/Early Triassic; mTr/eTrl: Middle Triassic/early Late Triassic; lTrm/lTr: late Middle Triassic/Late Triassic; lTr/eJ: Late Triassic/Early Jurassic; eJ: Early Jurassic.

the Triassic portion of the West Gondwana APWP, where part (~25°) of the rotation evidently occurred during the Neogene (Muttoni *et al.* 1995)[1] (Fig. 8). The Neogene rotation was tentatively interpreted by Muttoni *et al.* (1995) in the framework of a complex history of local tectonic rotations, sometimes in opposite senses in adjacent blocks, that have occurred since the Early Miocene in the northeastern Aegean and western Anatolia (Kissel *et al.* 1987; see also Kissel *et al.* 1989). The pre-Neogene component of rotation was tentatively associated with the Korabi–Pelagonian microplate rifting as Chios moved independently of both West Gondwana and Laurussia (Muttoni *et al.* 1995). However, no such palaeomagnetic evidence for the Korabi–Pelagonian microplate rifting can be drawn from the Kçira data, assuming that all the clockwise rotation at Kçira occurred during the Neogene. Thus, either the pre-Neogene rotation at Chios was not related to the Triassic rifting of the Korabi–Pelagonian microplate, or Chios was tectonically separated from Kçira, and the Korabi–Pelagonian microplate did not move as a single tectonic unit.

ACKNOWLEDGMENTS

Field work in northern Albania was made possible by a cooperative agreement between the Faculty of Geology and Mines of the Polytechnical University of Tirana (Albania) and the Earth Science Department of the University of Milan (Italy). Palaeomagnetic analysis was conducted at the palaeomagnetics laboratory of Lamont-Doherty (USA) supported by US NSF grant ATM93-17227. This study was partially funded by the Centro di Geodinamica Alpina e Quaternaria of the Consiglio Nazionale delle Ricerche d'Italia. Lamont-Doherty Earth Observatory contribution 5549.

[1] *Errata corrige* in Muttoni *et al.* (1995): the Early/Middle Triassic boundary palaeopole for Chios shows a counterclockwise rotation of 67° with respect to the Triassic palaeopoles from West Gondwana (in northwest Africa coordinates) and of 111° with respect to those from Laurussia (in European coordinates), and not *vice versa*, as reported in the text by these authors. We refer to Fig. 12 in Muttoni *et al.* (1995) for clarification.

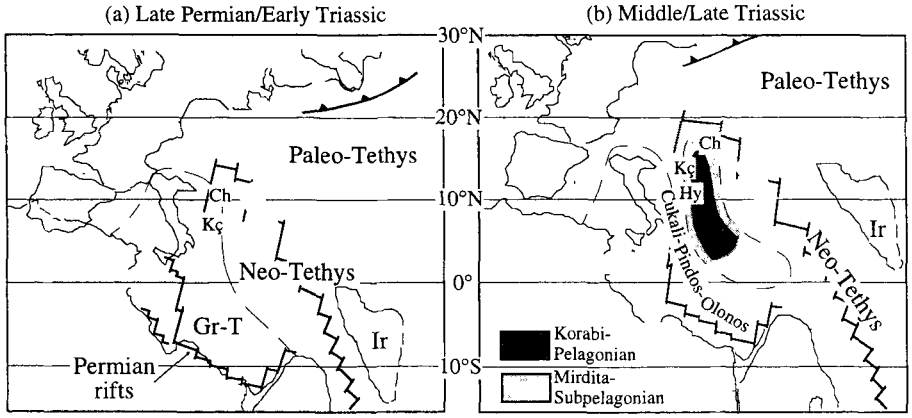

Figure 9. Paleogeographic reconstruction of the western portion of the Tethys during (a) Late Permian/Early Triassic, and (b) Middle/Late Triassic (both adapted from Muttoni *et al.* 1996). Ch is the Chios sections (Greece) (Muttoni *et al.* 1995); Gr-T is an unsubdivided Greco-Turkish unit; Hy is the Middle Triassic Aghia Triada section (Greece) (Muttoni *et al.* 1994); Kç is Kçira (present study); and Ir is the Iran–Afghanistan–Mega Lhasa unit(s).

REFERENCES

Arthaber, von G., 1911. Die Trias von Albanien, *Beitr. Paläont. Geol. Österreich-Ungarns,* **24,** 169–277.

Beccaluva, L. *et al.*, 1994. A cross section through western and eastern ophiolitic belts of Albania, Working Group meeting, IGCP Project no. 256—Field trip A, *Ofioliti,* **19/1,** 3–26.

Gaetani, M., Jacobshagen, V., Nicora, A., Kauffmann, G., Tselepidis, V., Sestini, N.F., Mertmann, D. & Skourtsis-Coroneou, V., 1992. The Early–Middle Triassic boundary at Chios (Greece), *Riv. It. Paleont. Strat.,* **98,** 181–204.

Gallet, Y., Besse, J., Krystyn, L., Marcoux, J. & Theveniaut, H., 1992. Magnetostratigraphy of the Late Triassic Bolucektasi Tepe section (southwestern Turkey): Implications for changes in magnetic reversal frequency, *Phys. Earth planet. Inter.,* **73,** 85–108.

Gallet, Y., Besse, J., Krystyn, L., Theveniaut, H. & Marcoux, J., 1993. Magnetostratigraphy of the Kavur Tepe section (southwestern Turkey): A magnetic polarity time scale for the Norian, *Earth planet. Sci. Lett.,* **117,** 443–456.

Gallet, Y., Besse, J., Krystyn, L., Theveniaut, H. & Marcoux, J., 1994. Magnetostratigraphy of the Mayerling section (Austria) and Erenkolu Mezarlik (Turkey) section: Improvement of the Carnian (Late Triassic) magnetic polarity time scale, *Earth planet. Sci. Lett.,* **125,** 173–191.

Godroli, M., 1992. Tectonique des ophiolites dans les Albanides internes: modalites d'ouverture et de fermeture d'un bassin oceanique etroit (exemple des ophiolites de la zone de Mirdita), *PhD thesis,* Universite de Paris-Sud, centre d'Orsay, France.

Graziano, S. & Ogg, J.G., 1994. Lower Triassic magnetostratigraphy in the Dolomites region (Italy) and correlation to Arctic ammonite zones, *Am. geophys. Un. Fall Meeting,* **75,** San Francisco, CA.

ISPGJ–ISGJN, 1982. *Gijeologjia e Shqiperise (Geology of Albania),* Tirana, Albania.

ISPGJ–ISGJN, 1983. *Harta Gijelogjike e Shqiperise (Geological map of Albania)*, Scale 1 : 200.000, Tirana, Albania.

Kellici, I., De Wever, P. & Kodra, A., 1994. Mesozoic radiolarians from different sections of the Mirdita nappe, Albania. Paleontology and stratigraphy. *Revue de Micropaleontologie,* **37,** 209–222.

Kent, D.V., Olsen, P.E. & Witte, W.K., 1995. Late Triassic–earliest Jurassic geomagnetic polarity sequence and paleolatitudes from drill cores in the Newark rift basin, eastern North America, *J. geophys. Res.,* **100,** 14 965–14 998.

Kirschvink, J.L., 1980. The least-squares line and plane and the analysis of palaeomagnetic data, *Geophys. J. R. astr. Soc.,* **62,** 699–718.

Kissel, C., Laj, C., Sengor, A.M.C. & Poisson, A., 1987. Paleomagnetic evidence for rotation in opposite sense of adjacent blocks in north-eastern Aegea and western Anatolia, *Geophys. Res. Lett.,* **14,** 907–910.

Kissel, C., Laj, C., Mazaud, A., Poisson, A., Savascin, Y., Simeakis, K., Fraissinet, C. & Mercier, J.L., 1989. Paleomagnetic study of the Neogene formation of the Aegean area, in *Tectonic Evolution of the Tethyan Region,* pp. 137–157, ed. Sengör, A.M.C., Kluwer, Dordrecht, The Netherlands.

Kodra, A., 1987. Scheme of the paleogeographical and geotectonic development of inner Albanides during the Triassic and Jurassic, *Bul. shkenc. gjeol.,* **4,** 3–18.

Kodra, A., 1988. Rifting of the Mirdita's continental crust and the first stages of the oceanic opening during the Jurassic, *Bul. shkenc. gjeol.,* **4,** 3–14.

Kovacs, S. & Kozur, H., 1980. Stratigraphische Reichweite der wichtigsten Conodonten (ohne Zahnreihen–Conodonten) der Mittel- und Obertrias, *Geol. Palaont. Mitt. Innsbruck,* **10/2,** 42–78.

Kummel, B., 1969. Ammonoids of the Late Scythian (Lower Triassic), *Bull. Mus. Compar. Zool.,* **137,** 311–701.

Lowrie, W., 1990. Identification of ferromagnetic minerals in a rock by coercivity and unblocking temperature properties, *Geophys. Res. Lett.,* **17,** 159–162.

Mauritsch, H.J., Scholger, R., Bushati, S.L. & Ramiz, H., 1995. Palaeomagnetic results from southern Albania and their significance for the geodynamic evolution of the Dinarides, Albanides and Hellenides, *Tectonophysics,* **242,** 5–18.

McFadden, P.L. & Lowes, F.J., 1981. The discrimination of mean directions drawn from Fisher distributions, *Geophys. J. R. astr. Soc.,* **67,** 19–33.

McFadden, P.L. & McElhinny, M.W., 1990. Classification of the reversal test in palaeomagnetism, *Geophys. J. Int.,* **103,** 725–729.

Muttoni, G., Channell, J.E.T., Nicora, A. & Rettori, R., 1994. Magnetostratigraphy and biostratigraphy of an Anisian–Ladinian (Middle Triassic) boundary section from Hydra (Greece). *Palaeogeog. Palaeoclimat. Palaeoecol.,* **111,** 249–262.

Muttoni, G., Kent, D.V. & Gaetani, M., 1995. Magnetostratigraphy of a Lower–Middle Triassic boundary section from Chios (Greece), *Phys. Earth planet. Inter.,* **92,** 245–261.

Muttoni, G., Kent, D.V. & Channell, J.E.T., 1996. Evolution of Pangea: Paleomagnetic constraints from the Southern Alps, Italy, *Earth planet. Sci. Lett.,* **140,** 97–112.

Nicora, A., 1977. Lower Anisian platform conodonts from the Tethys and Nevada: taxonomic and stratigraphic Revision, *Palaeontographica,* **A-157,** 88–107.

Nopcsa, F., 1929. Geologie und Geographie Nordalbaniens, *Geol. Hungar. Soc. Geol.,* **3,** 1–620.

Orchard, M., 1995. Taxonomy and correlation of Lower Triassic (Spathian) segminate conodonts from Oman and revision of some species of *Neospathodus, J. Paleont.,* **69,** 110–122.

Robertson, A.H.F., Clift, P.D., Degnan, P.J. & Jones, G., 1991. Palaeogeographic and palaeotectonic evolution of the Eastern Mediteranean Neotethys, *Palaeogeog. Palaeoclimat. Palaeoecol.,* **87,** 289–343.

Shallo, M., 1992. Geological evolution of the Albanian ophiolites and their platform periphery, *Geol. Runds.,* **81,** 681–694.

Shallo, M., 1994. Outline of the Albanian ophiolites, *Ofioliti,* **19/1,** 57–75.

Speranza, F., Islami, I., Kissel, C. & Hyseni, A., 1995. Paleomagnetic evidence for Cenozoic clockwise rotation of the external Albanides, *Earth planet. Sci. Lett.,* **129,** 121–134.

Sweet, W.C., 1988. *The Conodonta,* Oxford monographs on Geology and Geophysics, **10,** Oxford University Press, Oxford.

Zijderveld, J.D.A., 1967. A.C. demagnetization of rocks—analysis of results, in *Methods in Paleomagnetism,* pp. 254–286, eds. Collinson, D.W., Creer, K.M. & Runcorn, S.K., New York, NY.